THE 4TH INTERNATIONAL CONFERENCE ON ALUMINUM ALLOYS

DEFORMATION MICROSTRUCTURES IN CHANNEL-DIE COMPRESSED ALUMINIUM CRYSTALS

J. H. Driver[1], D. Juul Jensen[2] and N. Hansen[2]

[1] Ecole des Mines de Saint Etienne, 158, Cours Fauriel, 42023 Saint-Etienne, France.
[2] Materials Department, Risø National Laboratory, 4000 Roskilde, Denmark

Abstract

High purity aluminium single crystals with orientations close to the stable rolling texture components of FCC metals, i.e., B $(110)[\bar{1}12]$, S $(213)[\bar{1}\bar{4}2]$ and C $(112)[11\bar{1}]$, have been channel-die compressed to a strain of one and the deformation substructures characterised on the longitudinal section by optical microscopy, TEM and SEM with EBSD.

All orientations exhibit a microstructure typical of cold-rolled polycrystals, i.e. dislocation cells, cell blocks, dense dislocation walls and ordinary microbands. The microband structure is shown to be composed of a regular, homogeneous and periodic array of elongated cells of average misorientation $\sim 2°$ with the microband plane inclined at $\sim 30°$ to 'RD'.

Only the microband structure is observed in the soft, double-slip, B orientation ; in the harder C and S crystals it is broken up by narrow bands of localized glide. The S orientation exhibits characteristic S-shaped band structures of first generation microbands sheared on the {111} planes of the dominant slip system. The C orientation develops non-crystallographic micro-shear bands. The processes of localized slip in the normally stable S and C orientations are associated with large local misorientations (10-15°) as a consequence of the heterogeneous flow. These orientations are stable in terms of average textures but clearly unstable in terms of microstructures.

Introduction

With the aim of quantitatively predicting the properties of plastically formed materials, the deformation structures in heavily deformed fcc metals have been extensively studied over the last decade. Thus studies of rolled aluminium [1], nickel [2] and copper [3] polycrystals have shown that the dislocation structures can be described in terms of two basic configurations [4]:

(i) At medium strain ($0.1 < \varepsilon < 0{,}5$) as cell blocks delineated by dense dislocation walls (DDWs) and first generation microbands (MB1s) which contain dislocation cells.

(ii) At very high strains ($\varepsilon > 2$) as lamellar structures composed of dislocation walls parallel to the rolling plane together with elongated subgrains.

However, a wide variety of dislocation structures have been observed in polycrystals of fcc metals deformed to strains in the transition region ($\varepsilon \approx 1$): equiaxed and elongated cells, microbands, cell blocks, lamellar structures and deformation, transition and shear bands. Given the inhomogeneity of plastic deformation that occurs within grains, and from grain to grain, the origin of these structures is difficult to determine in polycrystals. They can be characterised more rigorously using single crystals, of representative orientations, deformed to large strains under polyslip conditions, as in plane strain compression.

The purpose of this paper is to examine the influence of crystal orientation, and active slip systems, on the deformation microstructures of aluminium crystals deformed by channel-die compression into the transition stage region. They are representative of the usual fcc rolling texture components, namely {112} <111> (C), {110} <112> (B), and a {112} <174> (near-S) orientation.

The experimental methods of crystal preparation, sample testing and metallographic techniques have been described in detail in [5]. All micrographs and EBSD analyses were obtained on the longitudinal, RD/ND, plane.

Results

Macroscopic behaviour

As expected, the 'copper' C, $(112)[11\bar{1}]$ and 'Brass' B, $(110)[\bar{1}12]$ crystals are stable in channel die, as they are in rolling. Crystal S lies initially off the classical S orientation $\{123\}\langle 63\bar{4}\rangle$ but rotates about 15° towards a more stable S orientation $(213)[\bar{1}\bar{4}2]$. The stress states, active slip systems, finite strains and lattice rotation were calculated for the above orientations using a standard Taylor, Bishop and Hill rigid-plastic model and the appropriate boundary condition for channel die deformation (3 independent strain rate components). The calculated slip rates lead to ε_{13} and ε_{12} shear components that are in agreement with the macroscopic shape changes, i.e. large ε_{13} shears for crystals C and S and a large ε_{12} shear for the B orientation. The reference system used here is X_1=RD, X_2 = TD and X_3 = ND.

Deformation structures

Crystal B. Polarized light metallography of the stable (110)[112] orientation revealed a very homogeneous structure without any visible large misorientations. This was confirmed by an EBSD line scan along X_1, from which the local misorientations, $\Delta\theta$ were plotted out at 2μm intervals (Fig. 1a). The $\Delta\theta$ peaks have values of 2 to 6° and mean spacings ~5 μm. The rotation axes corresponding to the local misorientations are randomly distributed, figure 1b.

A typical dislocation structure fig.1c, consists of slightly elongated cells of dimension 1x2μm, aligned at about 30° to 'RD'. In this particular case, the dislocation cell walls are parallel to the trace of the (111) plane which is one of the 2 predominant slip systems. The general features are consistent with the dislocation structures previously observed by Chandra-Holm and Embury [6] on the compression face of this orientation.

The dislocation cells are grouped together into regions of roughly constant orientation, termed cell blocks, separated by dense dislocation walls (DDWs). This micrograph also shows examples of the characteristic splitting of DDWs into first generation microbands (MB1s). The cell blocks, of dimensions 5 to 10 μm, i.e. roughly 3 - 5 dislocation cell widths, are misoriented with respect to adjacent blocks by about 3 to 5^{o}. These TEM values correspond quite well to the X_1 spacings and the misorientations of the EBSD $\Delta\theta$ peaks.

Figure 1. Local misorientations $\Delta\theta$ along the X1 axis (a), rotation axes (b) and TEM microstructure (c), of B orientation at $\varepsilon = 1$. Spot size in (b) is proportional to $\Delta\theta$.

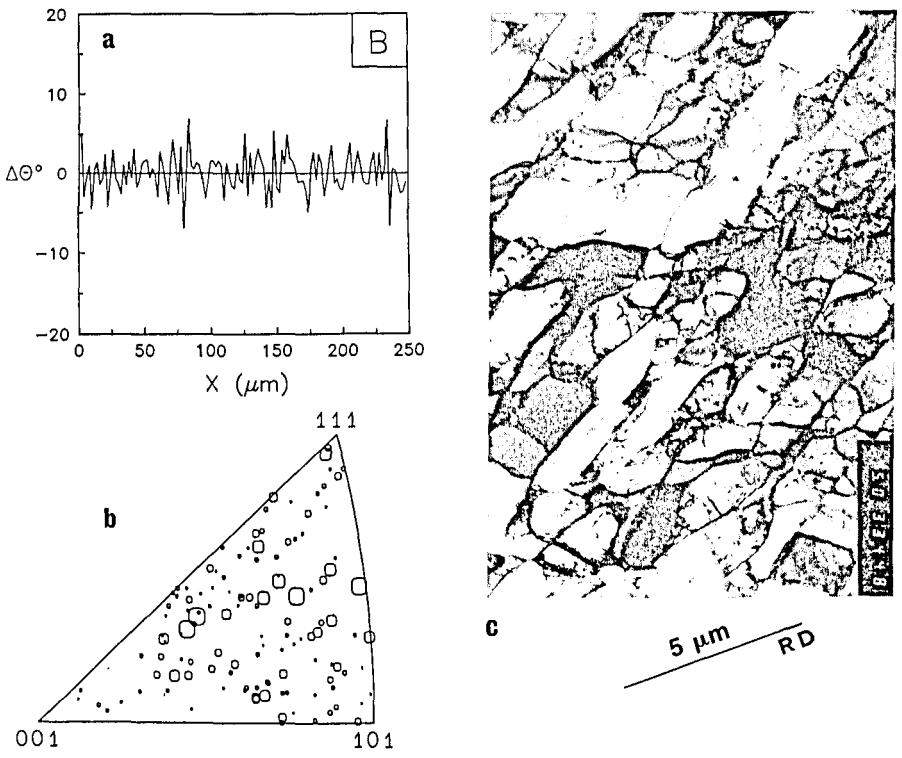

Crystal S. As shown in Figure 2 below, the $(123)[\bar{1}\bar{4}2]$ crystal developed a significantly different microstructure with two distinctive features:

(i) a regular pattern of elongated cells and MBs of spacing ~5 μm, inclined about 30^{o} to X_1

(ii) superimposed S bands with a coarser spacing making a fairly wide range of angles to RD (from 10^{o} to 25^{o}).

In this case, the local misorientations taken from an EBSD line scan along X_1 (Fig. 2a) are significantly higher than those of the B orientation. Apart from the usual 2 - 3^{o} misorientations

there are many $\Delta\theta$ peaks of ± 8 to 10^{o} with spacings of the order of ~ 20 μm. As before, however, the misorientation axes are fairly random, figure 2b.

The S-band structures are regions of localized shear by concentrated glide such that the matrix microbands are sheared into an S-shape as seen in 70% rolled polycrystalline aluminium [1] and nickel [2]. In the present case, they have widths of 1 to 10 μm, typically 2 μm, and make angles of about 10^{o} to 28^{o} to X_1. Most of the slip in this crystal takes place on the $(111)[01\bar{1}]$ system making an angle of $+25^{o}$ to X_1 (at $\varepsilon = 1$). The fact that the trace of the dominant (111) slip plane coincides with the upper range of the microshear band angles strongly suggests that these S-bands are bands of localized slip on crystallographic {111} planes, which on compression, undergo a rigid body rotation towards RD. The shear that takes place in the band centres is estimated from the MB1 displacement offsets as $\sim$ 1 to 3. Detailed TEM [5] also reveals a difference in structure between the high angle (new) S-bands and the low angle (old) bands. The high angle bands exhibit continuous curvature of the microband walls into a classical S. The lower angle bands show extensive 'pinching off' of the sheared microbands into paired dislocation walls aligned closer to 'RD'. Apparently, the S-band structure changes on subsequent deformation to fine, elongated cells nearly parallel to RD, in accordance with the suggestion [2] that they are precursors to the high strain lamellar structures.

Figure 2. Local misorientations $\Delta\theta$ along the X1 axis (a), rotation axes (b) and TEM microstructure (c), of S orientation at $\varepsilon = 1$. Spot size in (b) is proportional to $\Delta\theta$.

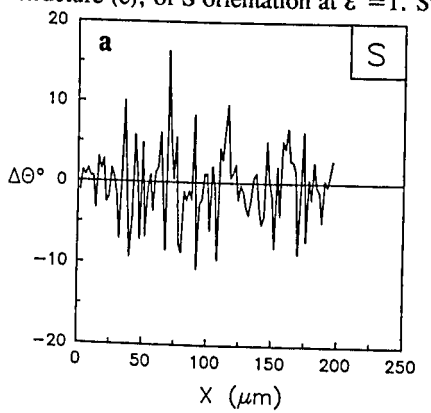

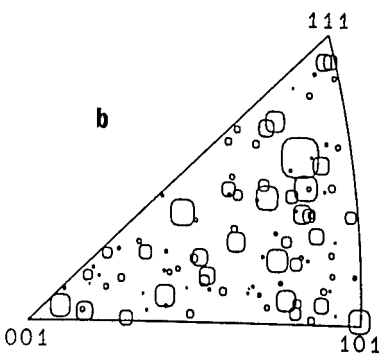

Crystal C. Another form of local shear process is found in the $(112)[11\bar{1}]$ orientation. At a strain of 1, the structure is composed of a very regular mixture of relatively large, slightly elongated, dislocation cells and MB1s (at a positive angle to X_1) and thin bands negatively inclined to X_1. The MB1s exhibit a typical periodic array of cells with a wide range of misorientations. The latter are characterized by the EBSD scan of Figure 3a showing that local misorientations up to $\pm 10^{o}$ occur frequently in this crystal. Note also that the rotation axes corresponding to the **large** misorientations, figure 3b, occur systematically about the <110> axis, i.e., the transverse direction whereas the small misorientations have a more random distribution. These large misorientations have irregular spacings of about 10 to 50 μm, which roughly correspond to the spacings of the fine bands seen by polarized light optical microscopy and by TEM. These bands are taken to be microshear bands in the sense of thin straight bands of shear along non-crystallographic planes. In the present case they are parallel to the (331) plane and could not have started as localized slip bands along a {111} slip plane (as in S). The nearest critically stressed slip plane (111) is closer to X_1(at 19°) and it is clearly impossible for a localized glide band to develop on such a plane and then rotate away from RD.

The microshear bands have a width of $\sim 1\mu$m and are composed of very elongated cells, typically 0,5 μm x 3 to 4 μm.. Close inspection reveals that they are associated with large offsets of the matrix MB1s; typical local shears in the bands seem to be of the order of 4 or 5.

Figure 3. Local misorientations $\Delta\theta$ along the X1 axis (a), rotation axes (b) and TEM microstructure (c), of C orientation at $\varepsilon = 1$. Spot size in (b) is proportional to $\Delta\theta$.

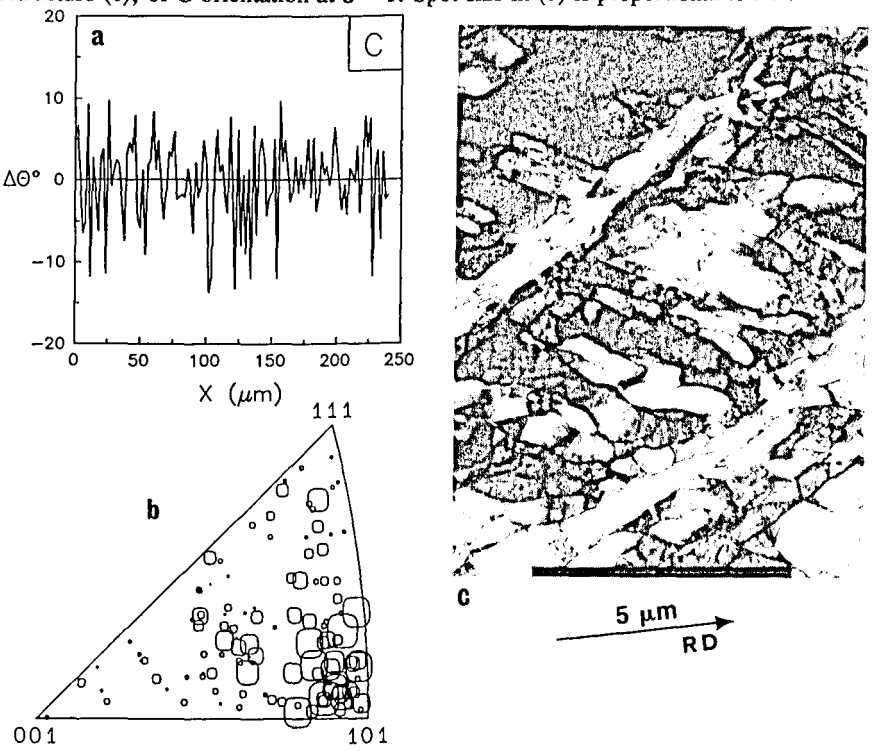

Discussion and Conclusions

An obvious, but important, result of the present work is that the dislocation structures in the channel die compressed crystals are, in general, very similar to those reported in high SFE fcc metals after rolling by reductions of 30 to 80% [1-3]. The most common feature is the presence of blocks bounded by dense dislocation walls and microbands. This structure is observed in all the crystals with a similar appearance, independent of crystal orientation. Besides this "typical" structure two types of characteristic bands are observed: bands of localized slip on {111} in the S orientation and micro-shear bands of non-crystallographic shear in the C orientation. They are revealed by both polarized light optical metallography and TEM and are associated with 'noisy' EBSD misorientation scans.

The orientation dependence of the microstructures in deformed crystals explains, at least in part, the variety of microstructures observed in grains of polycrystals deformed to this strain level. It also clearly suggests that oriented single crystals can be used to systematically characterize the evolution of particular types of microstructure- and their influence on recovery and recrystallization processes. The effect of orientation on microstructural development is treated in further detail in the following.

Cell blocks and Microbands

The microstructural subdivision into cell blocks has been discussed in previous papers [1-4] covering the behaviour of polycrystalline materials. In general this subdivision is favoured by a heterogeneous stress and strain distribution and by a tendency to minimize the flow stress by reducing the number of operating slip systems and thereby the number of intersecting jogs [4]. The deformation pattern of the three single crystals is quite homogeneous but apparently subdivision also takes place in this case; this may be caused by a tendency to minimise dislocation interactions. As an example, strong Lomer-Cottrell interactions are in fact expected in all the orientations tested here for the following slip system combinations:

C and S: $(111)[01\bar{1}] + (1\bar{1}1)[110]$, B: $(111)[\bar{1}01] + (11\bar{1})[011]$

Cell block formation arises then from the creation of volume elements which would minimise these reactions. It is probably impossible, given the requirements of strain compatibility, to completely eliminate them entirely in each volume element. In this case the blocks would slip on similar slip systems but with different slip amplitudes; this would lead to a progressive increase in misorientation without generating prohibitively high incompatibility stresses. Crystal subdivision into cell blocks would of course create some long range stresses but, in accordance with the LEDS (low energy dislocation structures) concept [7], these could be minimized by the development of periodic spatial configurations in mosaic patterns. There is substantial evidence from the present work that this occurs exclusively in single crystals as well as in polycrystals.

The dense dislocation walls/microbands make angles of $\sim 30^{o}$ to the 'rolling' direction; this is slightly lower than the average angle observed in polycrystals $\sim 40^{o}$ but is well within the

typical angular range. The walls coincide with slip plane traces in two orientations (B and C) but not in the S. No particular significance is attached to the coincidence of walls and slip traces since in most orientations at least one slip plane should be inclined in the range of 40 $\pm$ 10^{o} with respect to RD. In fact the fairly large and constant angle that the MB1s make with RD implies that they can rotate back against the rigid body rotation of material lines which tend to align them with RD. This confirms the view that this type of dislocation wall is easily rearranged in aluminium at room temperature.

The formation of cell blocks and microbands in previous papers has been discussed on the basis of the LEDS concept [1-5,7]. Two features characterizing such structures are also observed in the present study, namely the formation of alternating orientations giving rise to black and white contrast and the formation of rotational dislocation boundaries. This apparently easy formation of LEDS structures reflects the high moblity of dislocations in aluminium as discussed in the previous subsection.

Localized Glide Microstructures

The localized glide structures are bands which develop in the S and C orientations. The S, $(213)[\bar{1}\,\bar{4}2]$, crystal forms S shaped band morphologies as a consequence of localized shears, by concentrated slip, of the matrix MB1 structure. The range of angles that the S bands make with RD implies a continuous process of band nucleation along the dominant slip system $(111)[01\bar{1}]$ followed by rotation of the bands towards RD. Band structures have been reported by Kamijo et al. [8] in a $(348)[\bar{1}\,\bar{1}\,46]$ ($\sim$S) aluminium crystal rolled to a strain of 2.3. However, by TEM these authors did not observe S-band structures but rows of elongated cells. The observations of low angle, i.e. old, S-bands in the process of evolving to cell structures strongly suggests that the S-band configuration is a characteristic of the early stages of localized slip. This also fits in with previous observations of S-bands in Al [1] and Ni 2] polycrystals rolled to strains in the range 0,7 to 1,2.

As proposed in Ref.[2], the S-bands can reorganize the matrix MB1 structure so that the dislocation walls of the slip bands tend to realign the structure along RD.

The micro-shear bands observed in the C $(112)[11\bar{1}]$ orientation are unequivocal examples of non-crystallographic micro-shear bands in aluminium at room temperature. Given the well-defined angles of the possible slip traces in this stable orientation, only non-crystallographic shear can account for the microband traces. This is consistent with previous observations of micro-shear bands in rolled copper single crystals of C and S orientations [9]. The bands formed at a strain of unity may, however, be subsequently broken up by turbulent flow processes at higher strains since they were not observed by Morii et al. [10] in a rolled aluminium crystal of C orientation at ε =2.3

The present single crystal results throw some light on models of shear band nucleation at the grain level. The S and C orientations which developed localized glide have a common simple property, namely relatively high Taylor factors ($\sim$40% higher than the B crystal). They also

tend to have uneven slip distributions, particularly for the S orientation. The combination of high stresses, low work hardening rates and tendency to slip on one plane favours nucleation of bands of localized glide at relatively low strains. It is of course probable that other grain orientations during rolling develop bands of localized slip at some strain; the present work suggests that at least 2 of the common components of fcc rolling textures do so at a strain of the order of unity and no doubt with interesting consequences for recrystallization.

Acknowledgements

The authors wish to thank Mr. J. Lindbo for preparing the thin foils and Ms. Cl. Maurice for the programmes used to calculate the misorientation angles and axes.

References

1. B. Bay, N. Hansen and D. Kuhlmann-Wilsdorf, Mat. Sci. Eng. A158, (1992), 139.
2. D.A. Hughes and N. Hansen, Metall. Trans., 24A, (1993), 2021.
3. V.S. Ananthan, T. Leffers and N. Hansen, Mat. Sci. Tech. 7, (1991), 1069.
4. B. Bay, N. Hansen, D.A. Hughes and D. Kuhlmann-Wilsdorf, Acta Metall. Mater., 40, (1992), 205.
5. J.H. Driver, D. Juul Jensen and N. Hansen, Acta Metall. Mater. in press.
6. H. Chandra-Holm and J.D. Embury, Yield Flow and Fracture of Polycrystals, ed. T.N. Baker, (App. Sci. Publ., 1983), 275.
7. D. Kuhlmann-Wilsdorf, Mater. Sci. Eng. A113, (1989), 1.
8. T. Kamijo, A. Fujiwara and H. Inagaki, Scripta Metall. Mater. 25, (1991), 949.
9. K. Morii and Y. Nakayama, Proc. ICOTOM6, Vol. 1, ed. S. Nagashima, (1981), 327.
10. K. Morii, H. Mecking and Y. Nakayama, Acta Metall. 33 (1985), 379.